Characterization of the natural and forced recirculation bubble downstream a Backward-Facing Step using real-time optical flow velocimetry

J. PIMIENTA[a,b], A. GIANNOPOULOS[a,b], J-L. AIDER[a]

a.PMMH Laboratory, UMR 7636 CNRS, ESPCI Paris, PSL Research University, Sorbonne Université, Univ. Paris Diderot, 10 rue Vauquelin, Paris, France.

b. Photon Lines, 34 rue de la Croix de Fer, 78100, Saint-Germain-en-Laye, France

juan.pimienta@espci.fr, jean-luc.aider@espci.psl.eu

Résumé :

Des mesures par Particle Image Velocimetry en temps-réel (TR-PIV), basée sur un algorithme de flot optique, sont effectuées en aval d'une marche descendante. Cela permet de calculer en temps-réel l'aire instantanée de la bulle de recirculation de l'écoulement naturel dans un plan horizontal. L'évolution de l'aire de la bulle de reciruclation instantanée peut ainsi être engegistrée pendant des temps longs (plusieurs heures) à une fréquence relativement élevée (40 Hz). Plusieurs fréquences naturelles, y compris de très basses fréquences, sont ainsi déterminées. L'écoulement est ensuite contrôlé au moyen de Jet Vortex Generators continus ou pulsés. Les géométries des buses de sorties des jets permettent de générer des paires de tourbillons longitudinaux contrarotatifs qui viennent perturber la couche limite juste en amont de l'arête de la marche. Les mesures par TR-PIV permettent également une évaluation rapide de l'effet de la fréquence d'actionnement pour différents nombres de Reynolds ($Re_h = [1500 : 2000]$). Les résultats montrent que l'excitation de la couche limite en amont du bord, avec une fréquence d'actionnement proche de la fréquence de l'écoulement naturel, conduit à une forte réduction de la zone de recirculation (jusqu'à -60%) dans le plan d'observation.

Abstract :

Real-time Particle Image Velocimetry (TR-PIV) measurements, based on an optical flow algorithm, are performed downstream of a backward-facing step. This allows to calculate in real-time the instantaneous area of the recirculation bubble of the natural flow in a horizontal plane. The evolution of the instantaneous recirculation bubble area can thus be recorded for long periods (several hours) at a relatively high frequency (40 Hz). Several natural frequencies, including very low frequencies, are thus determined. The flow is then controlled by means of continuous or pulsed Jet Vortex Generators. The geometries of the jet outlets allow the generation of longitudinal counter-rotating vortex pairs which disturb the boundary layer just upstream of the step edge. TR-PIV measurements also allow a quick assessment of the effect of actuation frequency for different Reynolds numbers ($Re_h = [1500 : 2000]$). The results show that the excitation of the boundary layer upstream of the edge, with an actuation frequency close to the natural flow frequency, leads to a strong reduction of the recirculation area (up to -60%) in the observation plane.

Mots clefs: Flow control, Backward-Facing Step flow, Open-loop control, pulsed jets, shear flow, separated flows, jet vortex generators, optical flow, real-time measurements.

1 Introduction

Flow control aims at forcing particular characteristics of a fluid flow using specific perturbations induced by various actuators. It has been widely studied and applied in both academic configurations, like flow separation over simple airfoils or backward-facing steps, and industrial applications such as aeronautics [1, 2], ground transports [3, 4], motor sport [5], to mention a few. The control of separated flows is crucial to improve aerodynamics, especially to lower the drag and control the lift of a vehicle. The Backward-Facing Step (BFS) flow is a useful benchmark case due to its simple geometry leading to a fully separated boundary layer and to the creation of complex fluid structures [6, 7]. It allows a better comprehension of the dynamics of the flow and of the complex mechanisms leading to a fully 3D separated flow. It is then a good test-case for various flow control strategies applied to different properties of the flow. In many studies, the objective of the control was to reduce the mean size of the recirculation bubble created downstream of the BFS .

Many different actuators at different flow conditions have been tested in both simulations and experimental conditions. Among the most popular strategies, one can cite blowing at the step edge or vortex generators upstream of the BFS. For instance, Chun & Sung [8] used a thin slot at the step edge to force the shear layer with a pulsed spanwise jet. They found that the maximum reduction of the recirculation length was obtained for a pulsing frequency comparable to the shedding frequency of the separated shear layer. Emami-Naeini & al. [9] performed a model reduction for active flow control over a 2D BFS for low and high Reynolds numbers, using suction/blowing injectors at the wall of the step. Acoustic actuation has been studied by Becker & al. [10] in large eddy simulations (LES) and in an experimental wind tunnel, where the actuator was a homogeneous blowing through a transverse slot at the edge of the step. McQueen & al. [11] performed experimental measurements at high Reynolds number in a wind tunnel, where the actuators were eight speakers at the edge of the step inside a slot with a 45° angle to the free-stream. Succesfull control was also achieved using a spanwise homogenous slot and a pulsed actuation upstream of the BFS [12, 13]. On the other hand, jet vortex generators (JVG) have also been widely studied to control flow separations. Selby & al. [14] performed an experimental parametric study over a series of different JVG configurations and found that these could provide equivalent level to flow control, compared to slot blowing, over larger span-wise regions. Ultimately, Cambonie & Aider work[15, 16, 17] led to a higher comprehension of the interactions between counter-rotating jet vortex generators (CRJVG) and an incoming boundary layer by means of volumetric velocimetry measurements. Various jet geometries and configurations were tested, showing that some parameters are critical to control the formation of counter-rotating streamwise vortices which will strongly change the incoming boundary layer just upstream the step edge.

Similar studies have been performed in the past [18, 19] using different actuators and Reynolds numbers but in most cases the observation plane was the vertical symmetry plane as for the previously mentioned studies. This choice is justified when the actuation is also homogeneous along the transverse direction, as in the case of a spanwise slot. It is more arguable when the actuation used induces 3D perturbation, as

in the case of solid vortex generators [20, 21] or jet vortex generators [15].

In the present study, the observation plane is horizontal, in order to take into account the spanwise modulations induced by the set of jet vortex generators located upstream of the BFS. The study was limited to Reynolds numbers ranging from 1500 to 2000, and to one horizontal PIV plane close to the downstream lower wall where the instantaneous, spatially averaged, recirculation bubble could be monitored.

The data acquisition was performed using Real-Time Particle Image Velocimetry (RT-PIV) measurements based on an optical flow algorithm running on GPUs [22]. Using RT-PIV as a visual sensor, it allowed for the instantaneous evaluation of the recirculation area. Thanks to these measurements, it was possible to record the time-evolutions of the recirculation area over very long-times (up to two hours) in order to access to most of the characteristic frequencies, even the very low frequencies of the natural flow. Then the effect on the recirculation area of the spanwise modulation induced by the CRJVG together with specific temporal excitations of the boundary layer upstream the BFS could be studied.

2 Experimental setup

2.1 Hydrodynamic channel

Experiments have been carried out in a hydrodynamic channel in which the flow is driven by gravity, using a constant level water tank to ensure a pressure differential of $\Delta P = 0.3\ bar$. The maximum free-stream velocity $U_\infty = 22\ cm.s^{-1}$ leads to a maximum Reynolds number based on the step height of $Re_h = \frac{U_\infty * h}{\nu} \approx 3300$ for a water temperature of 21°.

The flow is stabilized by divergent and convergent sections separated by honeycombs, leading to a turbulence intensity lower than 1 %. A NACA 0020 profile is used to smoothly start a Blasius boundary layer over the flat plate, upstream of the BFS. The test section is $80\ cm$ long with a rectangular cross-section $w = 15\ cm$ wide and $H = 7\ cm$ high (Fig. 1). The height of the step h is $1.5\ cm$ leading to a vertical expansion ratio of $A_y = \frac{H}{H+h} = 0.82$.

The JVGs are located at $x = -2h$, upstream the edge of the step edge.

2.2 Continuous or Pulsed Counter-Rotating Jet Vortex Generators

We show on Fig. 2 a) the geometry of the jet nozzles (the flow goes from top to bottom of the image). Their interactions with the incoming boundary layer generate a set of streamwise counter-rotating vortices, as illustrated on Fig. 2 b) using streamwise velocity iso-surfaces. The 11 "v" shaped jets nozzles were made via 3D printing. This jet configurations showed promising results at controlling a flat-plate boundary layer [17]. The strongly 3D nature of the perturbations justifies the choice of monitoring the velocity field in an horizontal plane downstream the step edge.

A pressurized tank is used to control the jets velocity. A pneumatic valve, integrated inside the tank, controls the actuation amplitude and pulsing frequency. The overall experiment is monitored using a Labview code designed to control the pneumatic valve.

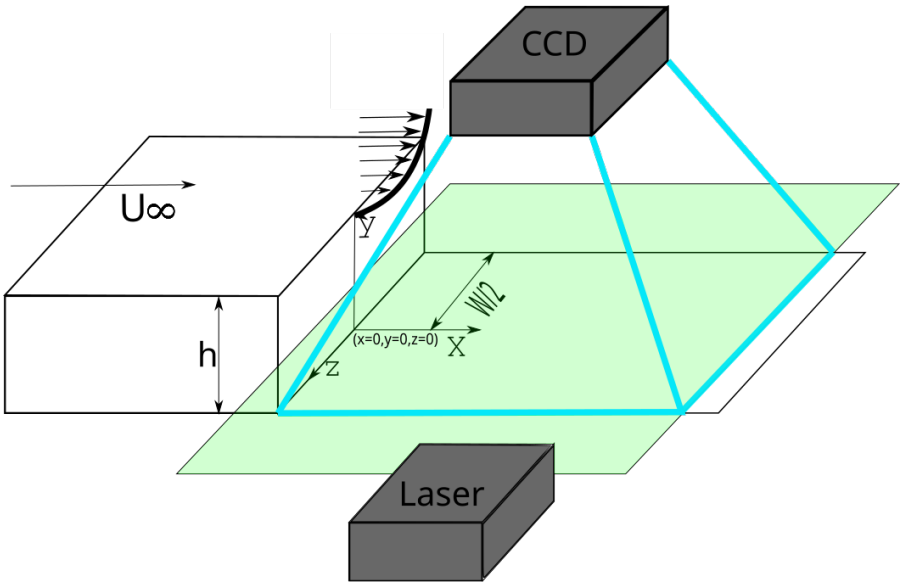


Figure 1: Sketch of the BFS together with the definition of the main parameters. The optical flow measurements were carried out in a horizontal plane, relatively close to the lower wall ($y = 0.3h$), just downstream the step.

2.3 Real-Time Optical Flow

The data acquisition was performed using Real-Time PIV inside a horizontal plane downstream of the step (Fig. 1). The laser sheet is generated by a continuous $1.5\ [w]$ Coherent laser beam operating at $\lambda = 532\ nm$ going through a Powell lens. The PIV snapshots are recorded using a PCO Panda.bi camera and streamed in real-time to a laptop with a dedicated GPU. The velocity fields and the instantaneous recirculation area were computed in real-time using an Optical-Flow PIV software [23, 24, 22, 25] (*EyePIV, Photon Lines*). Real-time measurements allowed for much longer data acquisition. In the present study, we could record instantaneous recirculation area over a very long time, giving access to both low and high frequencies. From a general point of view, RT-PIV gives access to more data leading to a better comprehension of both the natural and controlled flows.

3 Results

3.1 Natural flow

In this study the flow is characterized through the measurement of the recirculation area using real-time PIV. The instantaneous recirculation area of the fluid flow is defined as the sum of all the negative streamwise velocity vectors as shown in:

$$A_r(t) = \int_A H(-v(t))(x, y)dA \tag{1}$$

where $v(t)$ is the velocity vector, dA is the differential area, and H is full height of the experimental section upstream of the step. Usually this quantity is normalized by the square of the step height, h^2. In practice, this quantity was calculated as the total sum of pixels with negative streamwise velocity. This

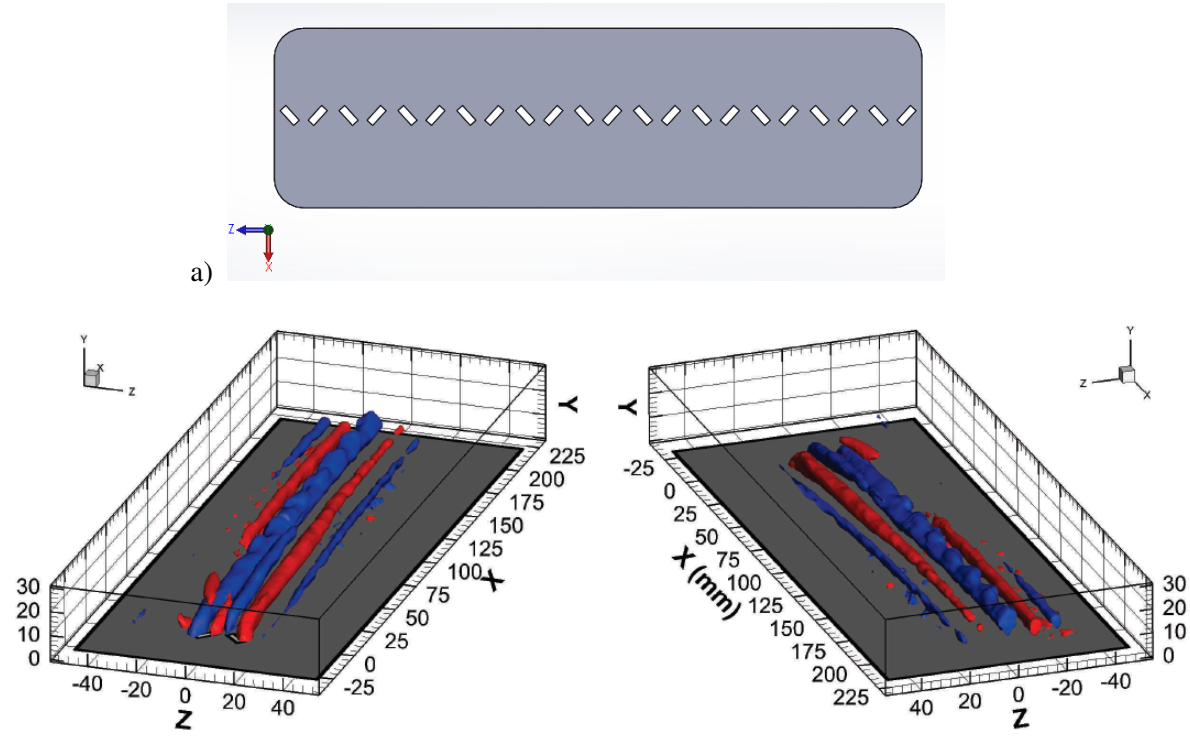


Figure 2: a) Geometry of the nozzle used to generate the counter-rotating jet vortex generators. b) Streamwise velocity contours obtained by 3D volumetric velocimetry showing the streamwise vortex created downstream the nozzles [17].

adds up to a scalar that is then converted to an area, multiplying by the pixel size of the image.

This calculation was performed in real-time, allowing to capture the fluctuations of $A_r(t)$, to later analyze the frequencies of the recirculation bubble by means of a power spectral density (PSD) of the time series of the RA. In a previous study [13], the vortex-shedding frequency for $Re_h = 2070$ and $Re_h = 2800$ were respectively $f_{sh} \approx 1.5\ Hz$ and $f_{sh} \approx 3\ Hz$. These frequencies were the most energetic found in the spectrum of local velocity fluctuations downstream the step edge, inside a vertical PIV plane. In the present study, low frequency peaks can be found in the PSD, which can be attributed to the Kelvin-Helmholtz spanwise vortex rolling, especially at $Re_h = 2000$, which is very close to the one found by Gautier & Aider [13], approximately at $1.5Hz$. We find $1.25Hz$ for $Re_h = 1700$ and $1.06\ Hz$ for $Re_h = 1500$. However, we observe other relevant frequencies around $10\ Hz$, and close to $19Hz$ (Figure 4).

3.2 Pulsed Controlled Flow

The measurements were also obtained using Real-Time PIV measurements, allowing for longer data acquisition times, and real-time computations of the recirculation area time-series. The time-series are 10 minutes long for each condition, natural flow, and controlled flow at frequencies $f = [1 : 4]\ Hz$.

Figure 5 presents the evolution of the dimensionless recirculation area as a function of time. In the first part of the time-series, we observe the evolution of the recirculation area of the natural flow. After approximately 2 min, the actuation is turned on. One can clearly see the sharp reduction of the recirculation area. The maximum reductions of the recirculation area were obtained with a frequency of $1\ Hz$ for each

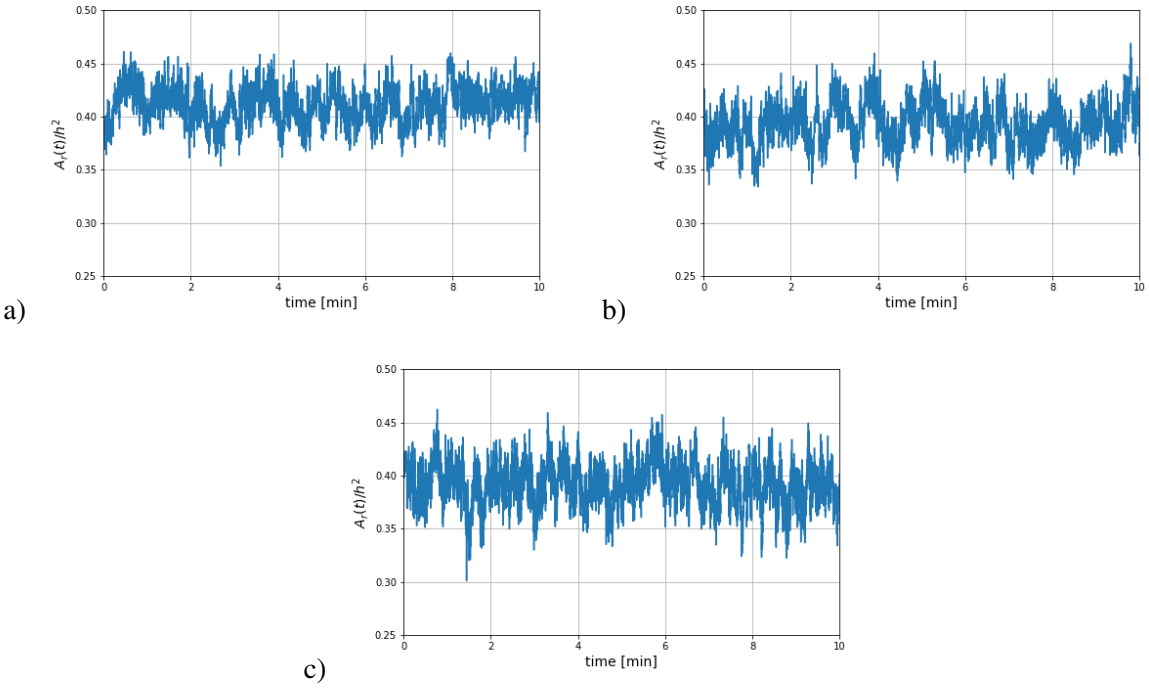


Figure 3: Natural flow - Time-series of the recirculation area at $y/h = 0.3$. a) $Re_h = 1500$. b) $Re_h = 1700$. c) $Re_h = 2000$.

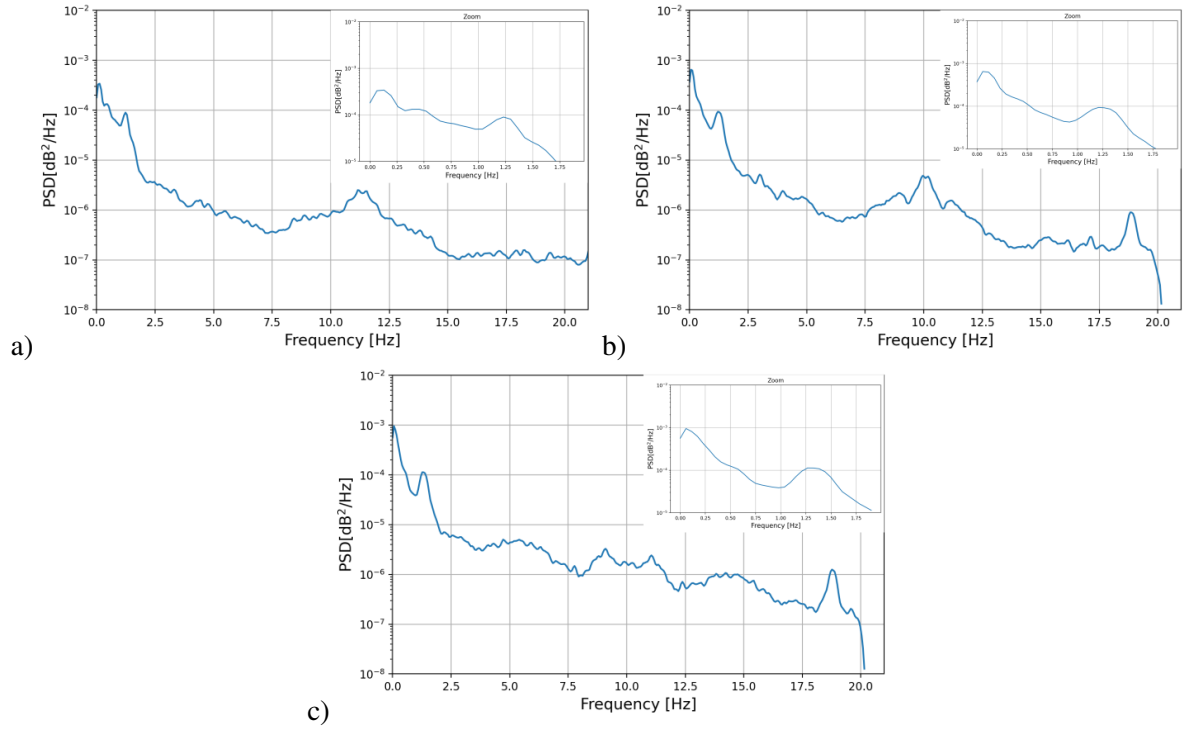


Figure 4: Natural flow - PSD of the time-series of the recirculation area at $y/h = 0.3$. a) $Re_h = 1500$. b) $Re_h = 1700$. c) $Re_h = 2000$. The inserts in the graphs show the same PSD zoomed in the range 0 to $1.75Hz$, to make the low frequencies more visible.

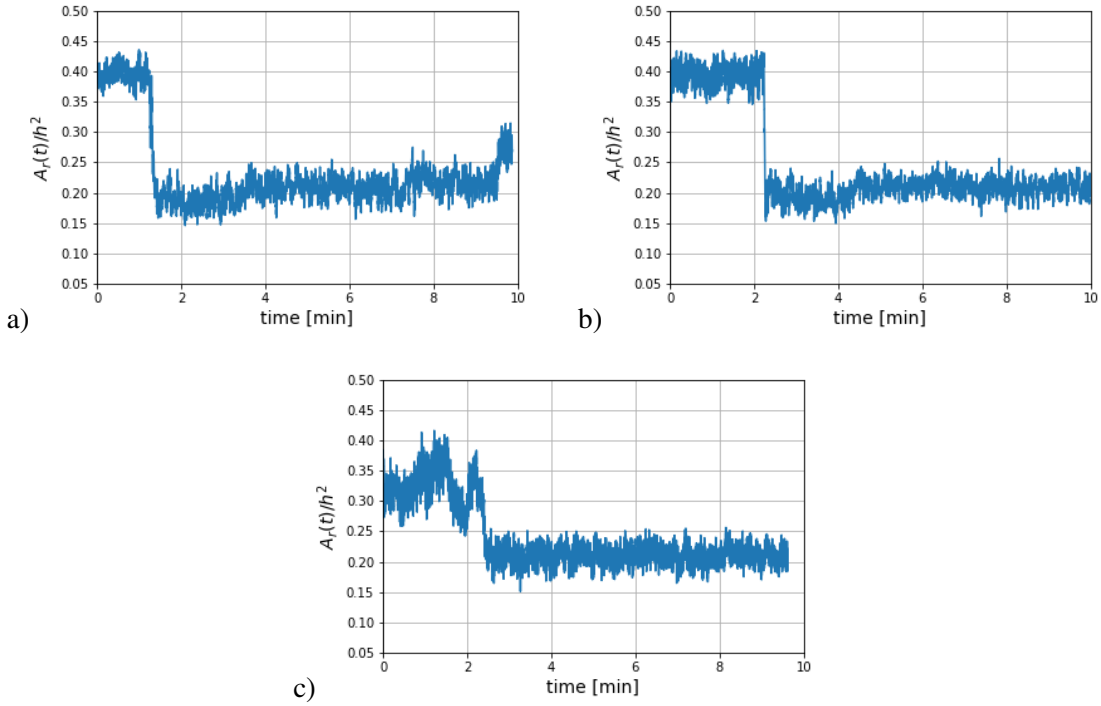


Figure 5: Pulsed actuation - Time series of the recirculation area at $y/h = 0.3$. a) $Re_h = 1500$. b) $Re_h = 1700$. c) $Re_h = 2000$.

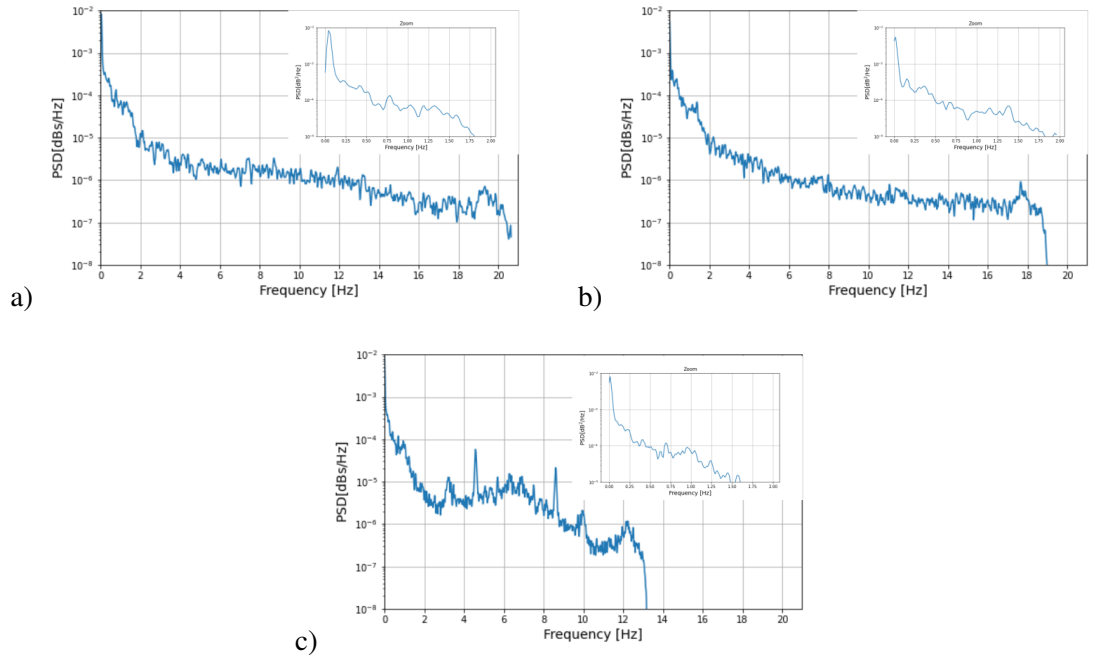
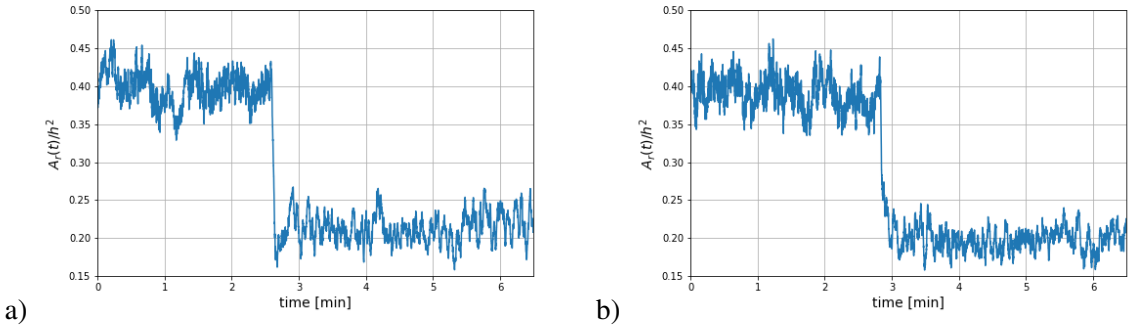


Figure 6: Pulsed actuation - PSD of the time series of the recirculation area at $y/h = 0.3$. a) $Re_h = 1500$. b) $Re_h = 1700$. c) $Re_h = 2000$. The inserts in the graphs show the same PSD zoomed in the range 0 to $1.75Hz$, to make the low frequencies more visible.

Reynolds number.

Figure 6 shows the PSD of the time-series of recirculation area. For $Re_h = 1500$ and $Re_h = 1700$ the PSDs no longer exhibit clear frequency peaks. For $Re_h = 2000$ there is a reorganization of the dominant frequencies. The dominant frequencies are around $4.5\ [Hz]$ and $8.5\ [Hz]$, while the dominant frequency of the natural flow are concentrated around $11\ Hz$. This general tendency of frequency reduction is found through the entire study between the pulsed controlled flow and the natural flow.



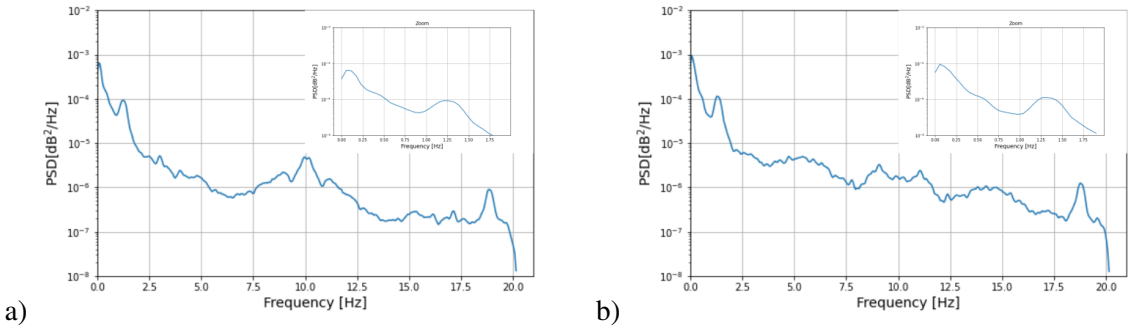
a) b)

Figure 7: Continuous actuation - Time series of the recirculation area at $y/h = 0.3$. a) $Re_h = 1700$. b) $Re_h = 2000$.

3.3 Continuous Controlled flow

Continuous control was then evaluated to discriminate between the effect of the spatial forcing by itself and the frequencies applied. As for the previous cases, measurements were performed with Real-Time PIV to extract the time-series of the recirculation area. Fig. 7 and Fig. 8 present the time-series and their PSDs. Here, the main point to remark is found on the PSD plots. Comparing Fig. 6 and Fig. 8 the main difference is the reduction of higher frequencies on the pulsed control case. For this continuous control case, the frequency spectrum is similar to that of the natural flow, even if the magnitude of the recirculation area was reduced approximately by 50%.

Finally, the effect of the pulsed and continuous actuations are compared in Fig. 9 for six Reynolds numbers, from 1500 to 2000. One can clearly see that the 1 Hz pulsed actuation is the most efficient in this range of Reynolds numbers.



a) b)

Figure 8: Continuous actuation - PSD of the time series of the recirculation area at $y/h = 0.3$. a) $Re_h = 1700$. b) $Re_h = 2000$. The inserts in the graphs show the same PSD zoomed in the range 0 to $1.75 Hz$, to make the low frequencies more visible.

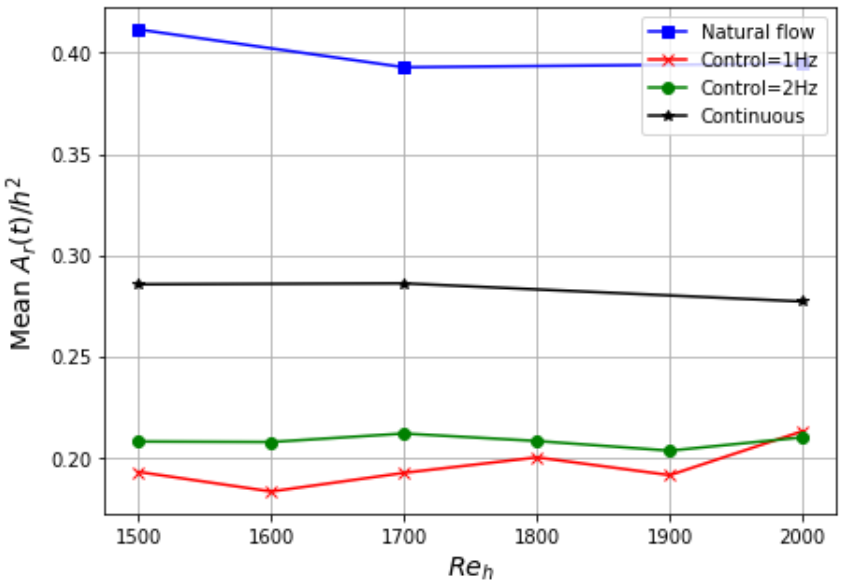


Figure 9: Comparison of the evolution of the time-averaged recirculation area in function of Re_h at $y/h = 0.3$.

4 Conclusion

In this study, we first characterized the time evolution of the instantaneous recirculation area downstream a backward-facing step. Using a new Real-time Optical Flow PIV system we were able to record long time series (2 hours in this case, but it could be as long as needed) of the recirculation area even with a relatively high sampling frequency (40 Hz). This type of measurement is made possible because the recirculation area is computed in the instantaneous PIV field in real time, and only one scalar ($A_r(t)$) is stored at each time step. It is then possible to have access to both very low (lower than 0.1 Hz) and high (up to 20 Hz) frequencies.

Open loop control was performed on the flow over the BFS by means of pulsed counter-rotating jet vortex generators.Because of their intrinsic 3D nature, we chose to characterize the flow in a given horizontal plane ($y/h = 0.3$) downstream of the BFS. Measurements were performed for three Reynolds numbers from $Re_h = [1500 : 2000]$. Jet actuation was carried out on two modes: continuous actuation and pulsed actuation. Pulsed jets were evaluated for frequencies ranging between 1 to 4 Hz. The most effective control, leading to the maximum reduction of the recirculation area, was the pulsed counter-rotating jet vortex generators at 1 Hz, with a mean reduction close to 60%, for an actuation frequency close to the most energetic frequency of the natural flow.

The continuous jet actuation case served to discriminate between the effect of the pure forcing of the jets and the pulsing effect. Although having indeed a significant effect, the reduction of the recirculation area was approximately -27%. The frequency analysis revealed the same dominant frequencies as in the natural flow.

The analysis of the frequencies revealed an important shift on the frequencies between the pulsed control and the natural flow, having an important effect on the reduction of higher frequencies and concentrating more energy on lower ones.

This study opens the path for further and more detailled analysis of the flow. Indeed, using Real-Time meaurements, it is now possible to monitor any scalar computed in real-time in instantaneous PIV fields.

It can record at the maximum acquisition frequency (more than 100 Hz, depending on the setup and the size of the sensor) over a very long time, giving access to a very wide spectrum. This approach also allows the application of various closed-loop flow control algorithm based on the visual sensor, either by targeting specific flow structures identified in the flow [13], or by feeding a data-base to find a proper and more sophisticated control algorithm [26].

References

[1] R. Sámano-Robles, J. Loureiro, E. Tovar, J. Viana, J. Cintra, and A. Rocha. Active flow control for aerospace operations by means of a dense wireless sensor and actuator network. *2016 IEEE 21st International Conference on Emerging Technologies and Factory Automation (ETFA)*, 2016.

[2] David Greenblatt and Israel J Wygnanski. The control of flow separation by periodic excitation. *Progress in aerospace Sciences*, 36(7):487–545, 2000.

[3] Zheng Hui, Xingjun Hu, Peng Guo, Zewei Wang, and Jingyu Wang. Separation flow control of a generic ground vehicle using an sdbd plasma actuator. *Energies, volume 12*, 2019.

[4] Jean-Luc Aider, Jean-François Beaudoin, and José Eduardo Wesfreid. Drag and lift reduction of a 3d bluff-body using active vortex generators. *Experiments in fluids*, 48(5):771–789, 2010.

[5] A.R.S. Azmi, A. Sapit, A. N. Mohammed, M. A. Razali, and N. Nordin A. Sadikin. Study on airflow characteristics of rear wing of f1 car. *IOP conf. Series: Materials Science and Engineering, volume 243*, 2017.

[6] Jean-Luc Aider, Alexandra Danet, and Marcel Lesieur. Large-eddy simulation applied to study the influence of upstream conditions on the time-dependant and averaged characteristics of a backward-facing step flow. *Journal of Turbulence, **8**, N51,*, 2007.

[7] Jean-François Beaudoin, Olivier Cadot, Jean-Luc Aider, and José Eduardo Wesfried. Three-dimensional stationary flow over a backward-facing step. *European Journal of Mechanics B/Fluids 23 147–155*, 2004.

[8] Kyung-Bin Chun and Hyung Jin Sung. Control of turbulent separated flow over a backward-facing step by local forcing. *Experiments in fluids*, 21(6):417–426, 1996.

[9] Abbas Emami-Naeini, Sarah A. McCabe, Dick de Roover, Jon L. Ebert, and Robert L. Kosut. Active control of flow over a backward-facing step. *Proceedings of the 44th IEEE Conference on Decision and Control, and the European Control Conference.*, 2005.

[10] Ralf Beck, Maiko Garwon, Carsten Gutknecht, Günter Bärwolff, and Rudibert King. Robust control of separated shear flows in simulation and experiment. *Journal of Process Control 15 (2005) 691–700*, 2005.

[11] Thomas McQuen, David Burton, John Sheridan, and Mark C. Thompson. Active control of flow over a backward-facing step at high reynolds numbers. *International Journal of Heat and Fluid Flow 93 (2022) 108891*, 2022.

[12] N Gautier and J-L Aider. Control of the separated flow downstream of a backward-facing step using visual feedback. *Proceedings of the Royal Society A: Mathematical, Physical and Engineering Sciences*, 469(2160):20130404, 2013.

[13] N Gautier and J-L Aider. Frequency-lock reactive control of a separated flow enabled by visual sensors. *Experiments in Fluids*, 56(1):1–10, 2015.

[14] G. V. Selby, J. C. Lin, and F. G. Howard. Control of low-speed turbulent separated flow using jet vortex generators. *Experiments in Fluids 12, 394-400*, 1992.

[15] T. Cambonie, N. Gautier, and J. L. Aider. Experimental study of counter-rotating vortex pair trajectories induced by a round jet in cross-flow at low velocity ratios. *Experiments in Fluids*, 54(3):1475, 2013.

[16] Tristan Cambonie and Jean-Luc Aider. Transition scenario of the round jet in crossflow topology at low velocity ratios. *Physics of Fluids*, 26(8):084101, 2014.

[17] Tristan Cambonie. *Étude par vélocimétrie volumique d'un jet dans un écoulement transverse à faibles ratios de vitesses*. PhD thesis, Université Pierre et Marie Curie - Paris VI, 2012.

[18] Nicolas Gauthier and Jean-Luc Aider. Upstream open loop control of the recirculation area downstream of a backward-facing step. *C. R. Mecanique 342, 382–388*, 2014.

[19] Nicolas Gautier and Jean-Luc Aider. Frequency-lock reactive control of a separated flow enabled by visual sensors. *Experiments in Fluids volume 56, Article number: 16*.

[20] Thomas Duriez, Jean-Luc Aider, and Jose Eduardo Wesfreid. Base flow modification by streamwise vortices: application to the control of separated flows. In *Fluids Engineering Division Summer Meeting*, volume 47519, pages 791–796, 2006.

[21] Thomas Duriez, Jean-Luc Aider, and José Eduardo Wesfreid. Self-sustaining process through streak generation in a flat-plate boundary layer. *Physical review letters*, 103(14):144502, 2009.

[22] Nicolas Gautier and JL Aider. Real-time planar flow velocity measurements using an optical flow algorithm implemented on gpu. *Journal of Visualization*, 18(2):277–286, 2015.

[23] Brian G. Schunck Berthold K.P. Horn. Determinig optical flow. *Atificial Intelligence Laboratory, Massachusetts Institue of Technology*, 1981.

[24] F. Champagnat, A. Plyer, G. Le besnerais, B. Leclaire, S. Davoust, and Y. Le sant. Fast and accurate piv computation using highly parallel iterative correlation maximization. *Exp Fluids, 50: 116-1182*, 2011.

[25] Antonios Giannopoulos, Pierre-Yves Passaggia, Nicolas Mazellier, and Jean-Luc Aider. On the optimal window size in optical flow and cross-correlation in particle image velocimetry: application to turbulent flows. *Experiments in Fluids*, 63(3):1–18, 2022.

[26] Nicolas Gautier, J-L Aider, THOMAS Duriez, BR Noack, Marc Segond, and Markus Abel. Closed-loop separation control using machine learning. *Journal of Fluid Mechanics*, 770:442–457, 2015.